Experimental study and sensing applications of polarization dependent Lossy Mode Resonances generated by D-shape coated optical fibers

P. Zubiate, C. R. Zamarreño, I. Del Villar, I.R. Matias, *Senior Member, IEEE*, F.J. Arregui

***Abstract*—The fabrication and characterization of an optical fiber refractometer based on Lossy Mode Resonances (LMR) is presented. TiO_2/ poly (sodium 4-styrenesulfonate) (PSS) coatings deposited on side-polished D-shaped optical fibers are used as LMR supporting coatings. LMRs are sensitive to the external medium refractive index and D-shaped optical fibers enable the observation of TE and TM LMR polarizations. These refractometers based on TE and TM LMR showed an average sensitivity of 2737 nm/RIU and 2893 nm/RIU respectively for a surrounding medium refractive index (SMRI) range from 1.35 to 1.41. This work also explores the utilization of previously described refractometers in the context of two common industrial applications such as the determination of the sugar content or °Brix in beverages and the salt concentration in sea water.**

***Index Terms*—D-shaped, LMR, Optical fiber, Refractive index, Refractometer, Sugar content, Salinity concentration TiO_2/PSS.**

I. Introduction

A great number of contributions related to the optical fiber sensors have been analyzed and reported extensively, during the last decades [1-4]. Optical fiber sensors present many advantages over other sensing technologies such as electromagnetic immunity, small size, light weight, low cost, low transmission losses or wavelength multiplexing. The utilization of optical fiber sensors for detection of different elements or analyses has been addressed by different authors in literature using a wide range of interrogation techniques, such as those based on interferometry [5], long-period gratings [6], fiber Bragg gratings [7] or resonances [8].

When an optical waveguide is coated by a thin-film, the propagation of light is affected and different types of resonances can be observed attending to the dielectric properties of the thin-films [9]. The most well-known phenomenon is surface plasmon resonance (SPR) [10]. This phenomenon occurs when the real part of the thin-film permittivity is negative and higher in magnitude than both its own imaginary part and the permittivity of the material surrounding the thin-film. Thus, SPRs are generated by TM polarized light and can be obtained with conducting materials, typically noble metals [11] . A different and not very exploited type of resonance is known as Lossy Mode Resonance (LMRs) [9],[12],[13]. This type of resonances occurs when the real part of the thin-film permittivity is positive and higher in magnitude than its own imaginary part and the real part of the permittivity of both the optical waveguide and that of the external medium surrounding the thin-film[14],[15].

In addition LMRs are generated by both TM and TE polarized light which can produce two differentiated LMRs (LMR_{TM} and LMR_{TE}) positioned at different wavelengths as it has been theoretically [13]and experimentally [16] demonstrated in previous works. Moreover, LMRs can be achieved with materials with low imaginary part of the refractive index, such as metal oxides like indium tin oxide (ITO) [17],[18], TiO_2[19], indium oxide and even polymers [20].

Here, it is described the generation of LMRs using metal/oxide/polymer coatings fabricated onto D-shaped optical fibers as well as the separation and characterization of the polarization dependent LMRs (LMR_{TM} and LMR_{TE}).

Additionally this work also presents the utilization of the described optical fiber device for refractive index, ºBrix and salinity sensing applications.

II. Experimental

A. Coating Fabrication

Titanium oxide (TiO_2) nanoparticles and poly (sodium 4-styrenesulfonate) (PSS) coatings were fabricated onto D – shaped optical fibers (purchased from Phoenix Photonics LTD) using the layer-by-layer (LbL) self-assembly technique [19]. LbL is based on electrostatic attractions and consists of the sequential adsorption of oppositely charged molecules. A PSS water solution (10 mM) was used as the anionic polyelectrolyte and a solution of TiO_2 in ultrapure water (10 mM) was used as the cationic solution. The pH of both anionic and cationic solutions was adjusted to 2.0 in order to promote the film adsorption. The D-shaped optical fiber was first immersed in 1 M KOH during 10 minutes and then washed in ultrapure water in order to acquire a prior negative charge. Once the substrate was negatively charged, it was immersed in the TiO_2 nanoparticles solution and then in a PSS solution for

Manuscript submitted September 5, 2014.

This work was supported by the Spanish Economy and Competitiveness Ministry-Feder TEC2013-43679-R Research Grant. The authors would like to express their gratitude to Nadetech Inc. for the tune-up of the robot used for the deposition of the nanocoatings. Special thanks to AIN for the utilization of the SEM and Nadetech for the laboratory equipment.

The authors are with the Electrical and Electronic Engineering Department, Public University of Navarra, 31006 Pamplona, Spain (e-mail: pablo.zubiate@unavarra.es;carlos.ruiz@unavarra.es; ignacio.delvillar@unavarra.es; parregui@unavarra.es; natxo@unavarra.es)

2 minutes each. The fiber was rinsed repeatedly in ultrapure water between these two immersion steps. The structure obtained after this process is known as bilayer and it is repeated until the required thickness or number of bilayer is obtained. D-shaped fibers [16] consisted of standard single mode fibers (Corning® SMF-28) with a cladding/core diameter of 125/7 µm and a polished length of 1.7 cm. these fibers were polished until obtaining an attenuation of 15 dB at 1550 nm in high index oil (1.5).

B. Fabrication and Measurement Setup

The experimental fabrication setup is shown in Fig. 1. This setup consisted of a multi-LED light (HP83437A) source with an emission spectrum between 1150 and 1680 nm and connected to a light scrambler in order to remove the polarization dependence of the light source. The depolarizer output is then connected to one end of the D-shaped fiber. The other end is connected to an optical spectrum analyzer (OSA-HP86142A). This setup is used to monitor the growth of the film and the wavelength shift of the LMRs as a function of the number of bilayers (thickness of the coating). The absorbance spectra are collected after each bilayer. The polarization of the light is not controlled during the fabrication. Therefore, the light used for the fabrication monitoring is not polarized.

Absorbance measurements at a certain wavelength of light (λ), were obtained from eq. (1):

$$A_\lambda(dB) = 10log_{10}\frac{I_0}{I} \qquad (1)$$

where I is the output intensity of light at a specified wavelength λ, when the light has passed through TiO_2/PSS coated D-shaped fiber immersed in different RI solutions (transmitted light intensity) and I_0 is the reference signal obtained at the output of a D-shaped fiber in air without any deposited coating

In order to guarantee the repeatability of the experiments, the climatic conditions were stabilized at 23 °C of temperature and relative humidity of 35 % during the fabrication process.

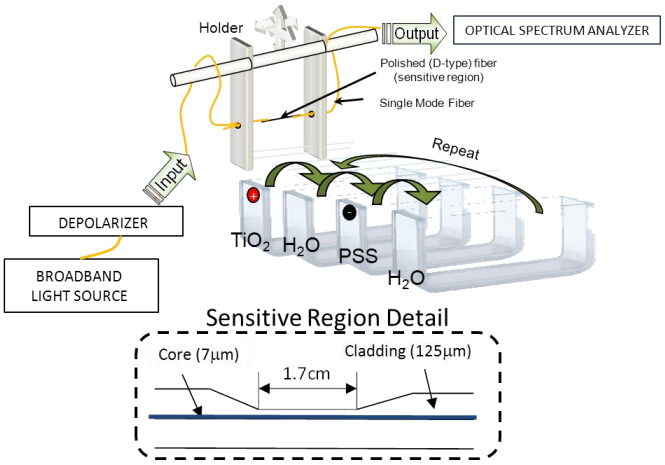

Fig. 1. Optical transmission setup (top) and sensitive region detail (bottom).

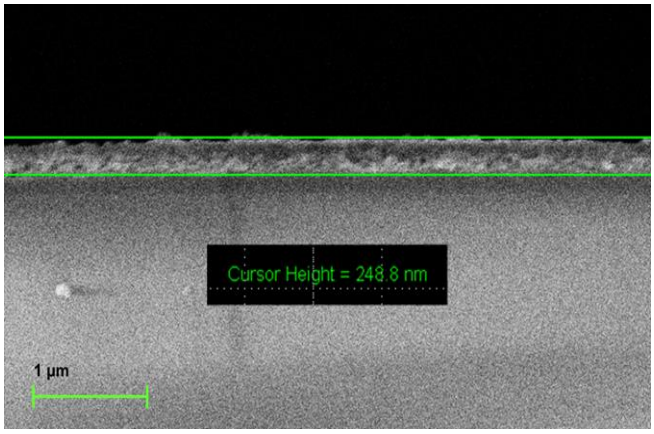

Fig. 2. SEM image of a TiO_2/PSS coating deposited on to the optical fiber core with thickness of 248.8 nm.

SEM images of the TiO_2/PSS coatings deposited onto the optical fiber core were obtained in order to guarantee the fabrication of homogeneous thin-films. Fig. 2 shows a TiO_2/PSS fabricated onto the optical fiber core with a thickness of 248.8 nm corresponding to a fabrication of 10 bilayers.

C. Characterization setup

After the fabrication of the TiO_2/PSS multilayer structure, a polarization control setup is used to separate and characterize the TM and TE components of the LMR (see Fig. 3). This setup consisted of a multi-LED light source (HP83437A) connected to a depolarizer (from Phoenix Photonics) in order to scramble the polarization of the light source. The depolarizer output is connected to a polarization controller (Agilent 9169A) and then to the TiO_2/PSS coated D-shaped fiber. The output is monitored using an OSA (HP-86142A). The characteristic asymmetry of the planar region of D-shaped fiber enables to differentiate between TM and TE polarizations and permits to obtain separately the LMRs associated with both polarizations LMR_{TM} and LMR_{TE}.

This setup was also used to characterize the device when it is subjected to changes in the external medium refractive index. The refractometric response of the device is obtained when the sensitive region is immersed into different aqueous glycerol solutions with different refractive index (RI): 1.35, 1.365, 1.38, 1.395, and 1.408. In the same manner, sugar content or Brix degree (ºBx) sensitivity is obtained when the sensitive region is immersed in solutions with different ºBx (19.5º, 29.9º, 39.6º, 45.5º). Here, ºBx denotes the sugar content of an aqueous solution. One ºBx is 1 gram of sucrose dissolved in 100 grams of solution and represents the strength of the solution as percentage by weight (% w/w). Finally, in order to test the salinity, the TiO_2/PSS coated region is immersed in salt-water solution with different concentrations: 16.90%, 21.10%, 23.50%, and 27%. The refractive index, ºBx and salinity of the test solutions were measured with the refractometer 30GS from METTLER TOLEDO Inc.

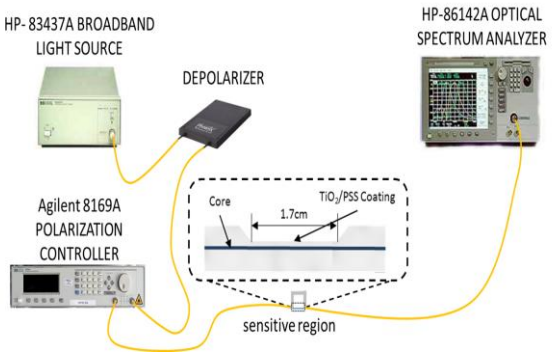

Fig. 3. Experimental measuring setup with the light source, the depolarizer the polarization controller and the detector and detail TiO_2/PSS coated sensitive region.

III. Results

A. Characterization of the TiO_2/PSS sensor

Fig. 4 shows the evolution of the LMR absorbance as a function of the number of bilayers added onto the D-shape fiber. Similar results can be observed in [19] were cladding-removed plastic-cladding silica fiber with 200μm core diameter is coated with up to 72 TiO_2/PSS bilayers. From Figure 4 it can be observed a first absorbance maximum at the very beginning of the fabrication process (between bilayers 2 and 4), which corresponds to the first LMR. The next absorbance maximum (2nd LMR) begins at bilayer 17th (1100nm) and ends at bilayer 26th (1700) with a total wavelength shift of 600 nm in 10 bilayers. The first LMR shifts faster than the second LMR as it has been already observed in previous works with TiO_2 and other materials [13, 16], revealing that the first LMR is more sensitive to coating thickness variations and also to external refractive index.

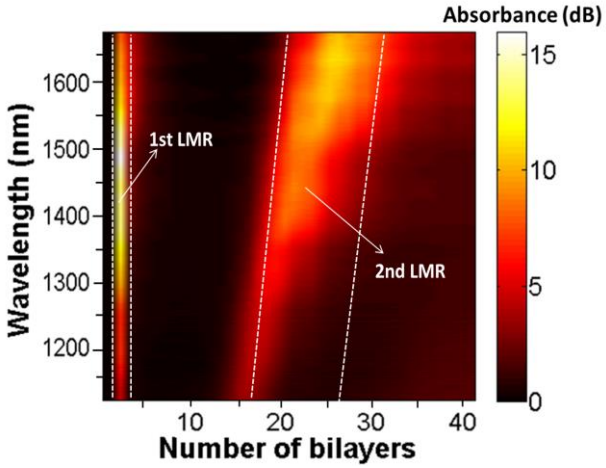

Fig. 4. Evolution of the transmitted spectra during the deposition of TiO_2/PSS coating.

The transmission spectrum of the first LMR after the deposition of 3 bilayers (when the sensitive region is in air, n=1) was obtained using the setup shown in Fig. 1 as it is shown in Fig. 5 (solid black line). Similarly the transmission spectrum of the second LMR after the deposition of 5 bilayers, when the sensitive region immersed in a 60% aqueous glycerol solution (n=1.38) is shown in Fig. 6 (solid black line). In this case, it is required the fabrication of a device with 5 bilayers in order to position the LMR within the studied region when the SMRI is 1.38 RIU.

In Fig. 5, the resonance wavelength of the first LMR is located at 1487 nm and the resonance wavelength of the second LMR, see Fig. 6, is located at 1341 nm. If we compare Figs. 5 and 6, the first LMR is broader and deeper than the second LMR. Since, previous works [13, 16] describe that both the first and second LMRs are formed by the contribution of TM and TE polarization resonance modes it could be assumed that in this case, the LMR_{TM} and LMR_{TE} contributions should be more distant, in wavelength, for the first LMR than for the second LMR.

B. TM-TE Polarizations

The separation of TM and TE resonance modes for the first and second LMRs is represented in Figs. 5 and 6, respectively (LMR_{TM} and LMR_{TE} are the dotted red line and the dashed blue line respectively). LMR_{TM} and LMR_{TE} can be obtained using the setup shown in Fig. 3.

The first LMR (see Fig. 5) has been separated in LMR_{TM} (dotted red line) and LMR_{TE} (dashed blue line). LMR_{TM} and LMR_{TE} wavelengths are located at 1364 and 1590 nm respectively with a separation between them of 226 nm. In Fig. 6 it is represented the separation of the second LMR in its components, LMR_{TM} (dotted red line) and LMR_{TE} (dashed blue line). In the case of the second LMR, maximum absorbance wavelengths are located at 1292 and 1381 nm for the LMR_{TM} and LMR_{TE} respectively, with a separation between them of 89 nm.

As it was assumed in the previous section, in the first resonance, the polarizations modes (LMR_{TM} and LMR_{TE}) are more separated than the second resonance. Moreover, it is demonstrated that the LMRs occur TM and TE polarized light.

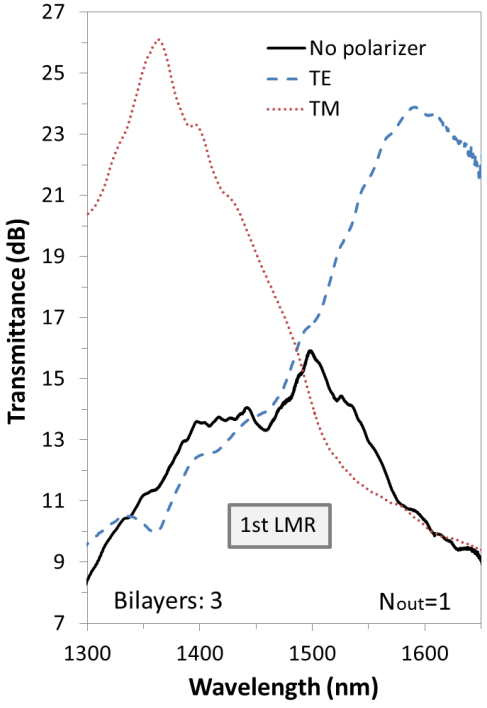

Fig. 5. Transmittance spectra of the first LMR using non-polarized light (solid black line), TM polarized light (dotted red line) and TE polarized light (dashed blue line).

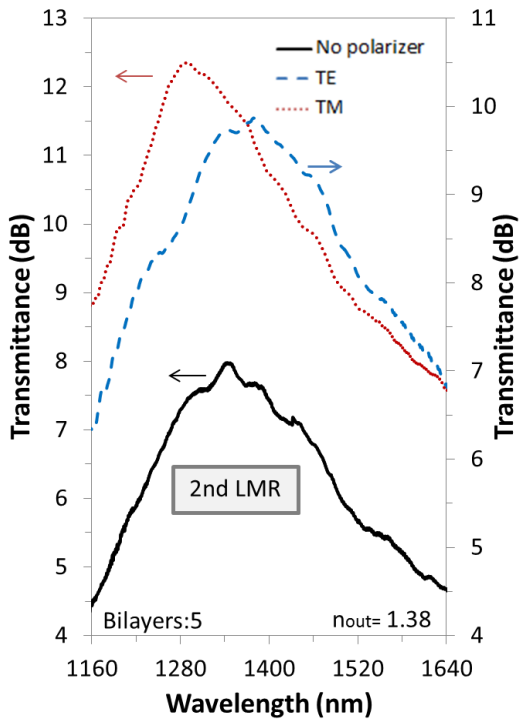

Fig. 6. Transmittance spectra of the second LMR using non-polarized light (solid black line), TM polarized light (dotted red line) and TE polarized light (dashed blue line).

C. *Applications*

Refractometers are widely used devices in many industrial applications such as agriculture, viticulture and sugar industry to measure °Bx (sugar content) or the study of sea water in order to measure salinity. In particular, LMR wavelength shift is associated to SMRI variations, which enable the fabrication of highly sensitive and robust refractometers based on wavelength measurement as it has been described in some of our previous works [17-19].

In order to check the experimental sensitivity of the device and its applications, the sensitive region of a device has been immersed in different solutions and the generated absorbance spectra were captured. The device under test was obtained after the fabrication of 3 bilayers of TiO_2/PSS under the conditions described before.

The applications of the device, described in the next sections, include the study of the refractometric response, the ºBx and the salt-content sensitivity.

1) *Refractometer*

LMR_{TM} and LMR_{TE} sensitivity as a function of the index refractive external was characterized experimentally by immersing the sensitive region in different aqueous glycerol solutions (20%, 30%, 40%, 50%, and 60%) with RI values of 1.35, 1.365, 1.38, 1.395, and 1.408. The response of both LMR_{TM} and LMR_{TE} to the SMRI variations is plotted in Figs. 7a and 7b respectively. The maximum absorbance wavelength of both resonances is shifted when subjected to different refractive index. Each resonance shifts to higher wavelengths when the RI value increases.

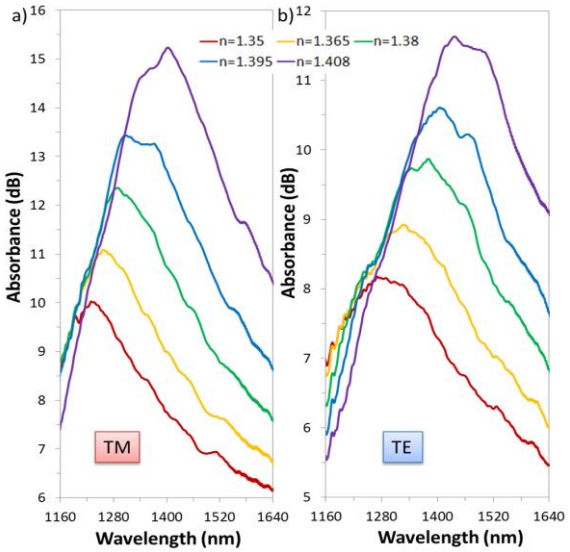

Fig. 7. Spectral response of the LMR_{TM} a) and LMR_{TE} b) when the sensitive region is immersed in solutions with different RI.

The sensitivities of the LMR_{TM} and the LMR_{TE} are 2893 and 2737 nm/RIU respectively in the range from 1.35 to 1.408. The sensitivities of both LMRs are in the same order of magnitude with an average dynamic range of 170 nm in the RI range tested which means a resolution of ~$2.05x10^{-5}$ RI by using a conventional communications Optical Spectrum Analyzer (OSA) as it is shown in Fig. 8. Each experiment was repeated four times, and averaged, being obtained a maximum error bar for the measured wavelength shifts of ± 0.287 nm. Maximum absorbance wavelength peaks have been obtained using a least squares parabolic fit Matlab® algorithm, where the wavelength peak corresponds to the parabola vertex.

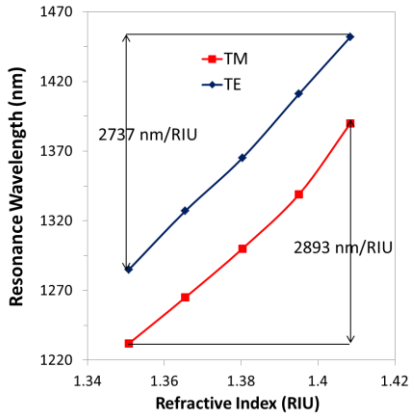

Fig. 8. Spectral position of the LMR band versus external refractive index.

2) *ºBx sensor*

A different application of the previously described device consists of the measurement of the ºBx. Measurement of ºBx is crucial in many applications, such as fruit juice, wine making, carbonated beverage industry and the sugar industry. LMR_{TM} and LMR_{TE} sensitivity as a function of the ºBx was characterized experimentally by immersing the sensitive region in different sugar-water solutions: 19.5 ºBx, 29.9 ºBx, 30.6 ºBx, 49,5 ºBx.

The response of LMR_{TM} to ºBx variations is shown in Fig. 9a. Here, it is important to note that as the ºBx or sugar concentration increases there is an optical wavelength shift of the resonance. In this plot it can be observed a wavelength shift of the resonance when the ºBx increases. The wavelength shift of the resonance central wavelength can be appreciated in Fig. 9b. In this case, the LMR experiments a shift of 158 nm (from 1222 nm when the ºBx is 19.5 to 1380 nm when the ºBx is 49.5). These values correspond to sensitivities of 5.2 nm/ºBx with good linear approximation (R^2 factor of 0.9787).

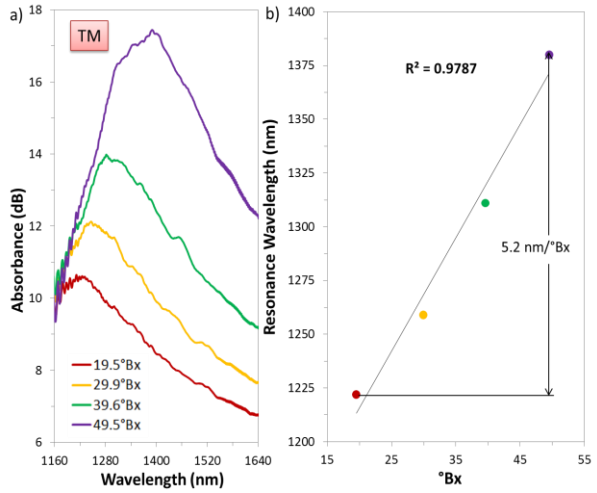

Fig. 9. a) Spectral response of the LMRTM and b) maximum attenuation wavelength for different °Bx.

In a similar way, the response of LMR_{TE} to ºBx variations is shown in Fig. 10a. In this plot it can be observed a wavelength shift of the resonance when the °Brix increases. The wavelength shift of the resonance central wavelength can be appreciated in Fig. 10b. In this case, the LMR experiments a shift of 151 nm (from 1278 nm when the ºBx is 19.5 to 1429 nm when the ºBx is 49.5°). These values correspond to sensitivities of 5 nm/ºBx with good linear approximation (R^2 factor of 0.9952).

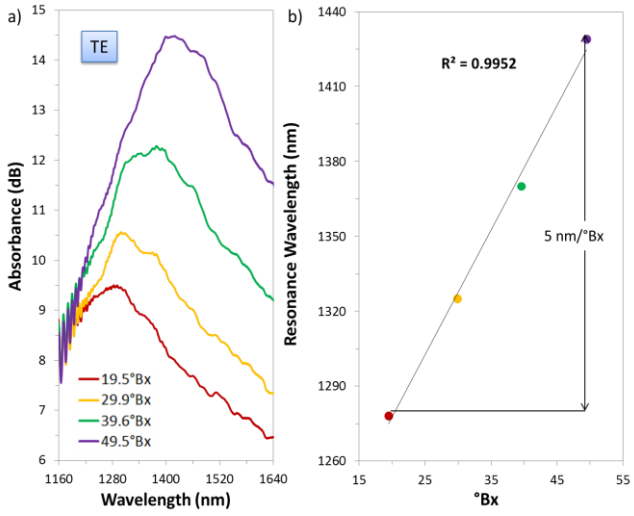

Fig. 10. Spectral response of the LMR_{TE} a) and maximum attenuation wavelength for different °Bx b).

The sensitivities of both LMRs (LMR_{TM} and LMR_{TE}) are in the same order of magnitude with an average dynamic range of 155 nm in the °Brix range tested which means a resolution of ~0.013 ºBx by using a conventional communications Optical Spectrum Analyzer (OSA). Each experiment was repeated four times, and averaged, being obtained a maximum error bar for the measured wavelength shifts of ± 0.214 nm

3) Salinity sensor

Salt content determination is another interesting application for this device. Salinity is one of the features of interest when studying the sea water. Therefore, control the level of salinity is important in many applications such as agricultural crops. As it was described in the previous section, in order to measure the salinity the coated region was immersed in different salt-water solutions: 16.9%, 21.10%, 23.50% and 27%.

The response of LMR_{TM} and LMR_{TE} to salinity variations is shown in Figs. 11a and 12a, respectively. Here, it can be appreciated that both the LMR_{TM} and LMR_{TE} central wavelength shift to the red when the device is introduced in solutions with increasing salt content.

The evolution of the LMR_{TM} central wavelength when the salinity is increased has been represented in Fig. 11b. In this case the LMR_{TM} experiments a shift of 38 nm (from 1204 nm when the salinity is 16.9% to 1242 nm when the salinity is 27%). These values correspond to sensitivities of 1122.7 nm/% with a good linear approximation (R^2 factor of 0.9896).

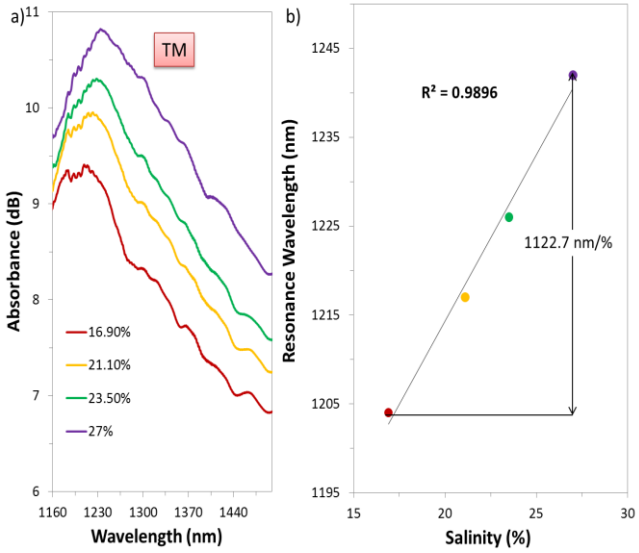

Fig. 11. Spectral response of the LMR_{TM} a) and maximum attenuation wavelength for different salt-water solutions b).

The evolution of the LMR_{TE} central wavelength when the salinity is increased has been represented in Fig. 12b. Here, the LMR experiments a shift of 35 nm (from 1256 nm when the salinity is 16.9% to 1301 nm when the salinity is 27%). These values correspond to sensitivities of 1176.6 nm/% with a good linear approximation (R^2 factor of 0.9976).

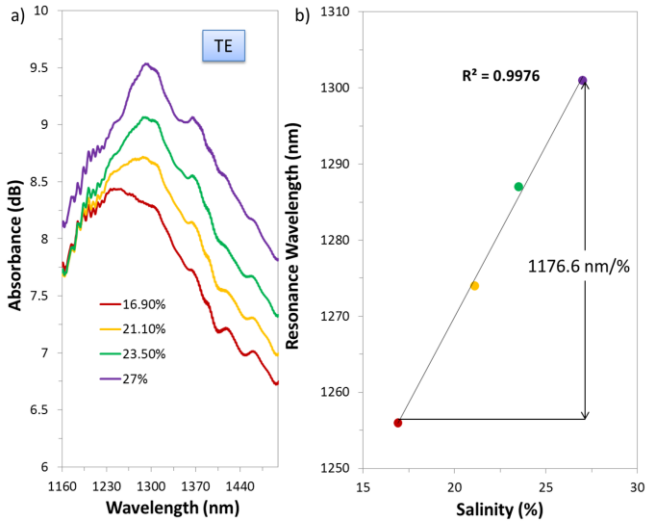

Fig. 12. Spectral response of the LMR_{TE} a) and maximum attenuation wavelength for different salt-water solutions b).

As happens in previous cases, the sensitivities of both LMRs (LMR_{TM} and LMR_{TE}) to salt content variations are in the same order of magnitude with an average dynamic range of 37 nm in the salinity range tested which means a resolution of ~0.015 % by using a conventional communications Optical Spectrum Analyzer (OSA). Each experiment was repeated four times, and averaged, being obtained a maximum error bar for the measured wavelength shifts of ± 0.268 nm

IV. Conclusions

LMR_{TM} and LMR_{TE} have been obtained by means of the fabrication of TiO_2/PSS coatings onto D-shaped SMF. The refractometric response of the LMR components (LMR_{TM} and LMR_{TE}) has been characterized for the first time to our knowledge. Both LMR_{TM} sensitivity (2893 nm/RIU) and LMR_{TE} sensitivity (2737 nm/RIU) are in the same order of magnitude within the studied RI range and comparable to commercial devices.

Fabricated devices have been also presented as suitable tools for ºBx and salt content measurement with good sensitivity and linearity within the studied range. Particularly, using a conventional communications optical spectrum analyzer (see figure 3), minimum variations of 2.05×10^{-5} RIU, 0.013 ºBx and 0.015 % of salinity could be resolved.

V. References

[1] B. Culshaw and A. Kersey, "Fiber-Optic Sensing: A Historical Perspective," *J. Light. Technol.*, vol. 26, no. 9, pp. 1064–1078, May 2008.

[2] O. S. Wolfbeis, "Fiber-Optic Chemical Sensors and Biosensors," *Anal. Chem.*, vol. 80, no. 12, pp. 4269–4283, 2008.

[3] A. Cusano, J. M. López-Higuera, I. R. Matias, and B. Culshaw "Optical Fiber Sensor Technology and Applications," *IEEE Sens. J.*, vol. 8, no. 7, pp. 1052–1054, 2008.

[4] T. L. Yeo, T. Sun, and K. T. V Grattan, "Fibre-optic sensor technologies for humidity and moisture measurement," *Sensors Actuators A Phys.*, vol. 144, no. 2, pp. 280–295, Jun. 2008.

[5] Z. Tian, S. S.-H. Yam, and H.-P. Loock, "Refractive index sensor based on an abrupt taper Michelson interferometer in a single-mode fiber," *Opt. Lett.*, vol. 33, no. 10, pp. 1105–1107, 2008.

[6] Y. Zhu, Z. He, and H. Du, "Detection of external refractive index change with high sensitivity using long-period gratings in photonic crystal fiber," *Sensors Actuators B Chem.*, vol. 131, no. 1, pp. 265–269, Apr. 2008.

[7] W. Liang, Y. Huang, Y. Xu, R. K. Lee, and A. Yariv, "Highly sensitive fiber Bragg grating refractive index sensors," *Appl. Phys. Lett.*, vol. 86, no. 15, p. -, 2005.

[8] R. C. Jorgenson and S. S. Yee, "A fiber-optic chemical sensor based on surface plasmon resonance," *Sensors Actuators B Chem.*, vol. 12, no. 3, pp. 213–220, Apr. 1993.

[9] F. Yang and J. R. Sambles, "Determination of the optical permittivity and thickness of absorbing films using long range modes," *J. Mod. Opt.*, vol. 44, no. 6, pp. 1155–1163, Jun. 1997.

[10] R. Slavík, J. Homola, and J. Čtyroký, "Single-mode optical fiber surface plasmon resonance sensor," *Sensors Actuators B Chem.*, vol. 54, no. 1–2, pp. 74–79, Jan. 1999.

[11] R. Slavik and J. Homola, "Novel surface plasmon resonance sensor based on singlemode optical fiber," vol. 3105, pp. 325–331.

[12] M. Marciniak, J. Grzegorzewski, and M. Szustakowski, "Analysis of lossy mode cut-off conditions in planar waveguides with semiconductor guiding layer," *IEE Proc. J Optoelectron.*, vol. 140, no. 4, p. 247, 1993.

[13] I. Del Villar, C. R. Zamarreño, M. Hernaez, F. J. Arregui, I. R. Matias, and S. Member, "Lossy Mode Resonance Generation With Indium-Tin-Oxide-Coated Optical Fibers for Sensing Applications," *J. Light. Technol.*, vol. 28, no. 1, pp. 111–117, 2010.

[14] I. Del Villar, C. R. Zamarreño, M. Hernaez, F. J. Arregui, I. R. Matias, and S. Member, "Lossy Mode Resonance Generation With Indium-Tin-Oxide-Coated Optical Fibers for Sensing Applications," vol. 28, no. 1, pp. 111–117, 2010.

[15] I. Del Villar, M. Hernaez, C. R. Zamarreño, P. Sánchez, C. Fernández-Valdivielso, F. J. Arregui, and I. R. Matias, "Design rules for lossy mode resonance based sensors," *Appl. Opt.*, vol. 51, no. 19, pp. 4298–4307, Jul. 2012.

[16] C. Ruiz Zamarreño, P. Zubiate, M. Sagües, I. R. Matias, and F. J. Arregui, "Experimental demonstration of lossy mode resonance generation for transverse-magnetic and transverse-electric polarizations.," *Opt. Lett.*, vol. 38, no. 14, pp. 2481–3, Jul. 2013.

[17] C. R. Zamarreño, I. Del Villar, P. Sanchez, M. Hernaez, C. Fernandez, I. R. Matias, and F. J. Arregui, "Lossy-mode resonance based refractometers by means of indium oxide coatings fabricated onto optical fibers," vol. 7653, pp. 1–4, 2010.

[18] C. R. Zamarreño, S. Lopez, M. Hernaez, I. Del Villar, I. R. Matias, and F. J. Arregui, "Resonance-based refractometric response of cladding-removed optical fibers with sputtered indium tin oxide coatings," *Sensors Actuators B Chem.*, vol. 175, pp. 106–110, Dec. 2012.

[19] M. Hernáez, I. Del Villar, C. R. Zamarreño, F. J. Arregui, and I. R. Matias, "Optical fiber refractometers based on lossy mode resonances supported by TiO 2 coatings," *Appl. Opt.*, vol. 49, no. 20, p. 3980, 2010.

[20] C. R. Zamarreño, M. Hernáez, I. Del Villar, I. R. Matías, and F. J. Arregui, "Optical fiber pH sensor based on lossy-mode resonances by means of thin polymeric coatings," *Sensors Actuators B Chem.*, vol. 155, no. 1, pp. 290–297, Jul. 2011.